

Aerosol Science and Technology

ISSN: 0278-6826 (Print) 1521-7388 (Online) Journal homepage: https://www.tandfonline.com/loi/uast20

Cyclone Collection Efficiency: Comparison of Experimental Results with Theoretical Predictions

John Dirgo & David Leith

To cite this article: John Dirgo & David Leith (1985) Cyclone Collection Efficiency: Comparison of Experimental Results with Theoretical Predictions, Aerosol Science and Technology, 4:4, 401-415, DOI: 10.1080/02786828508959066

To link to this article: https://doi.org/10.1080/02786828508959066

Published online: 06 Jun 2007.

Submit your article to this journal

Article views: 26258

View related articles

Citing articles: 107 View citing articles

Full Terms & Conditions of access and use can be found at
https://www.tandfonline.com/action/journalInformation?journalCode=uast20

Cyclone Collection Efficiency: Comparison of Experimental Results with Theoretical Predictions

John Dirgo* and David Leith†
Harvard School of Public Health, Physical Sciences and Engineering Program, 665 Huntington Avenue, Boston, MA 02115

This paper describes the results of tests conducted on a Stairmand high-efficiency cyclone. The cyclone was pilot-plant scale with a design air flow of 0.139 m^3/s (300 cfm). Collection efficiency and pressure drop were measured over a range of air flows at ambient temperature and pressure. An oil mist was used as a test aerosol because it consisted of spherical drops of uniform density unlikely to bounce or reentrain after striking the cyclone wall. At each air flow, a fractional efficiency curve (collection efficiency versus particle diameter) was determined. Experimental curves were compared with fractional efficiency curves generated by several cyclone efficiency theories. Over the range of particle sizes measured (1 to 7 μm), the predictions of a modified version of Barth's theory and the Leith–Licht theory were closest to experimental results.

NOMENCLATURE

a	cyclone inlet height, m
B	cyclone dust outlet diameter, m
b	cyclone inlet width, m
C	cyclone geometry parameter (dimensionless)
c_i	cyclone inlet dust concentration, kg/m^3
D	cyclone body diameter, m
D_e	cyclone gas outlet diameter, m
d	particle diameter, m
d_c	diameter of cyclone at natural length, m
d_{50}	cut particle diameter, collected with 50 percent efficiency, m
g	gravitational acceleration, m/s^2
H	cyclone height, m
h	cyclone cylinder height, m
h^*	height of cyclone core, m
l	natural length of cyclone, m
N	number of revolutions gas makes within the cyclone (dimensionless)
n	cyclone vortex exponent (dimensionless)
Q	volumetric gas flow, m^3/s
S	cyclone gas outlet duct length, m
T	absolute temperature, °K
v_i	gas inlet velocity, m/s
v_o	gas outlet velocity, m/s
v_t	tangential component of gas velocity in cyclone vortex, m/s
v_{ts}	particle terminal settling velocity, m/s
v_{ts}^*	terminal settling velocity of static particle, m/s
α	constant in Eq. (7) (dimensionless)
ΔH	cyclone pressure drop in inlet velocity heads (dimensionless)

**Current address*: PRC Engineering, 303 E. Wacker Drive, Chicago, IL 60601

†*Current address*: Department of Environmental Sciences and Engineering, School of Public Health, University of North Carolina, Chapel Hill, NC 27514

Aerosol Science and Technology 4:401–415 (1985)
© 1985 Elsevier Science Publishing Co., Inc.

0278-6826/85/$3.30

ΔP cyclone pressure drop in static pressure head, Pa

η fractional collection efficiency for particles of one size (dimensionless)

λ friction factor in Eq. (7) (dimensionless)

μ gas viscosity, Pa · s

ρ_g gas density, kg/m^3

ρ_p particle density, kg/m^3

Ψ cyclone inertia parameter (dimensionless)

INTRODUCTION

Cyclones have been used since the late 1800's to remove dust from industrial gas streams. Their simple design, low capital and maintenance costs, and adaptability to a wide range of operating conditions have made cyclones the most widely used industrial dust collectors. Because they rely on inertial forces to collect particles, cyclones have a low collection efficiency for particles smaller than about 5 μm in diameter. In spite of this disadvantage, there has been a renewed interest in cyclones, particularly in high-temperature, high-pressure applications such as fluidized bed combustion.

Many different types of cyclones have been built, but the reverse-flow cyclone with a tangential inlet (Figure 1) is most often used for industrial gas cleaning. This collector can be characterized by eight dimensions that are often expressed as their ratio to the cyclone body diameter, D. Table 1 shows the dimensions and dimension ratios for the Stairmand (1951) high-efficiency cyclone design used in this study. This design is one example of "standard" cyclone designs that have been developed. Many of these designs arose through a trial and error approach as "the result of 'hunches' or efforts to overcome operating difficulties" (Jackson, 1963).

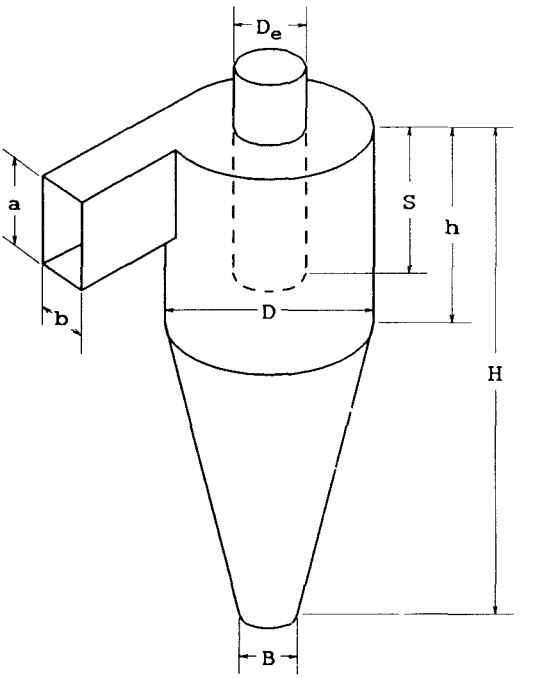


FIGURE 1. Reverse flow cyclone with dimensions.

TABLE 1. Dimensions of Stairmand High-Efficiency Cyclone Design

Dimension	Dimension ratio (dimension/D)	Length (m)
Cyclone diameter, D	1.000	0.305
Gas outlet diameter, D_e	0.500	0.152
Inlet height, a	0.500	0.152
Inlet width, b	0.200	0.061
Outlet duct length, S	0.500	0.152
Cyclone height, H	4.000	1.220
Cylinder height, h	1.500	0.457
Dust outlet diameter, B	0.375	0.114

According to Swift (1969), "...cyclones have been developed almost wholly by experiment, and it would be difficult to prove mathematically that [they] are of the best design..."

Although standard cyclone designs represent accepted engineering practice, there is no reason to assume that they provide the optimum possible performance. Cyclone theories can be used to predict changes in dimensions that should improve performance substantially. This paper presents the results of the initial phase of a study of improved cyclone design, in which fractional efficiency curves for a Stairmand high-efficiency cyclone were determined over a range of gas flow rates. The results will be used to evaluate the predictive capabilities of cyclone efficiency theories and to establish a "baseline" performance level for this cyclone. Later changes in performance due to changes in cyclone dimensions can be measured against this baseline.

THEORY

Cyclone collection efficiency, η, is defined as the fraction of particles of a given size that is retained by the cyclone. The theories that have been developed to predict efficiency differ greatly in complexity. There is a general agreement that operating parameters of the system should be used to predict performance, and most theories account for the influence of particle diameter and density, and gas velocity and viscosity. There is less agreement on the effects of cyclone dimensions and geometry. Some theories consider all eight cyclone dimensions while others include as few as three.

Separation of particles in the cyclone is due to the centrifugal force caused by the spinning gas stream; this force throws particles outward to the cyclone wall. Opposing this outward particle motion is an inward drag force caused by gas flowing toward the axis of the cyclone prior to discharge. All efficiency theories set up a balance between these opposing forces. By making different assumptions about gas flow through the cyclone, various terms in the force balance can be dismissed as insignificant. Since the relative importance of these terms will change with cyclone design and operating conditions, it is unlikely that any single set of assumptions will predict cyclone efficiency accurately for all applications. Leith (1979) has identified three general approaches to predicting cyclone collection efficiency; each is discussed below.

Critical Diameter: Timed Flight Approach

This method assumes that particles enter the cyclone a certain radial distance from the cyclone axis. Particles must travel outward from this position to the wall to be collected; the critical particle is the size that travels exactly this distance during its residence time in the cyclone. Different assumptions about initial radial position and residence time lead to different approximate solutions.

The Lapple (1950) cut diameter theory is the most widely used example of the timed flight approach. Lapple assumed that dust entering the cyclone was evenly distributed across the inlet opening. The particle size that travels from the inlet half width to the wall during the time in the cyclone is collected with 50% efficiency. Lapple calculated this particle size, the cut diameter, as

$$d_{50} = \sqrt{\frac{9\mu b}{2\pi\rho_p v_i N}} \tag{1}$$

Residence time is determined by the number of revolutions (N) the gas stream makes in the cyclone, each revolution covering a distance of πD. Lapple estimated $N = 5$ by determining the cut diameter experimentally and then solving Eq. (1) for N. Although he recommended experimental determination of N for different cyclones, his value is often used for all designs.

The efficiency for a particle of any size can be determined from its ratio to the cut diameter. Figure 2 is Lapple's curve of

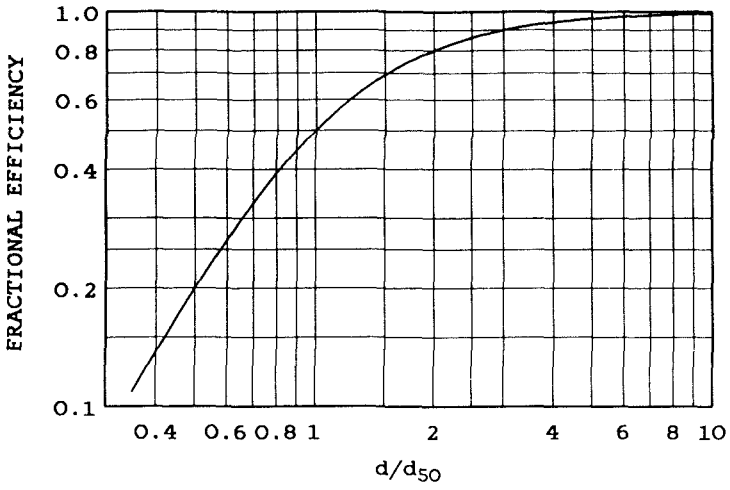


FIGURE 2. Fractional efficiency versus d/d_{50}, from Lapple (1950).

efficiency versus d/d_{50}. Theodore and DePaola (1980) have shown that the curve is described by

$$\eta = \frac{1}{\left[1 + (d/d_{50})^{-2}\right]}. \tag{2}$$

Figure 2 is based on Lapple's results from a single cyclone design and may not be valid for other configurations.

Critical Diameter: Static Particle Approach

The static particle approach determines the particle diameter for which centrifugal force is exactly balanced by the drag force. These particles should rotate indefinitely around the edge of the core, the central region of the cyclone below the gas outlet. Drag force on smaller particles exceeds centrifugal force so they are carried inward and out of the cyclone. Larger particles spin out toward the cyclone wall and are collected. The static particle approach predicts a sharp increase in cyclone efficiency from zero for particles smaller than the critical diameter to unity for larger particles. In practice, a sharp separation is never observed because of fluctuations in radial and tangential gas velocities over the height of the cyclone, and the efficiency for the critically sized particle is often assumed to be 50%.

Barth's (1956) efficiency theory, widely cited in European literature, is an example of the static particle approach. He defined the cyclone core as the imaginary cylindrical extension of the gas outlet down to the cyclone bottom or cone wall. Barth calculated the terminal settling velocity for the static particle as

$$v_{ts}^* = \frac{Qg}{2\pi h^* v_t^2}. \tag{3}$$

The collection efficiency for any other particle size is determined from the ratio of its settling velocity to v_{ts}^*.

$$\frac{v_{ts}}{v_{ts}^*} = \frac{\pi h^* v_t^2 \rho_p d^2}{9\mu Q}. \tag{4}$$

The height of the cyclone core is

$$h^* = H - S \quad \text{if} \quad D_e \le B, \tag{5}$$

$$h^* = \frac{(H-h)(D-D_e)}{(D-B)} + (h-S) \quad \text{if} \quad D_e > B. \tag{6}$$

Barth calculated the tangential gas velocity

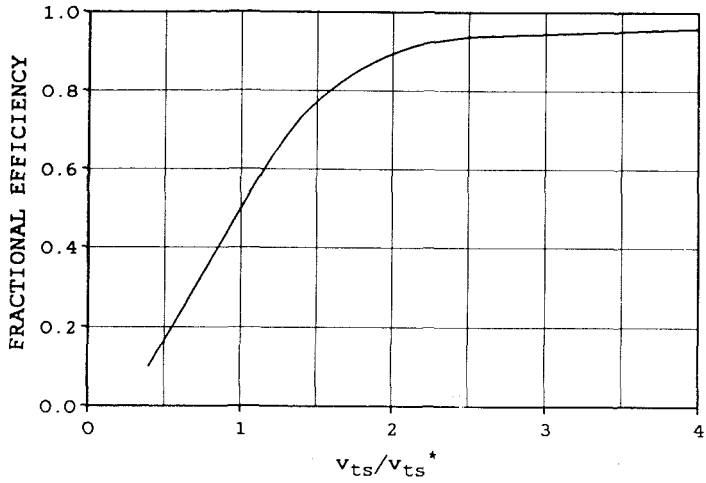


FIGURE 3. Fractional efficiency versus v_{ts}/v_{ts}^*, from Barth (1956).

at the edge of the cyclone core as

$$v_t = v_o\left[\frac{(D_e/2)(D-b)\pi}{2ab\alpha + h^*(D-b)\lambda\pi}\right], \tag{7}$$

where λ is a friction factor that Barth assumed to be 0.02 and

$$\alpha = 1 - 1.2(b/D). \tag{8}$$

Figure 3 is Barth's plot of efficiency versus the ratio v_{ts}/v_{ts}^*; it is based on experimental results for several cyclone designs. Barth's curve is closely approximated by

$$\eta = \frac{1}{\left[1 + \left(v_{ts}/v_{ts}^*\right)^{-3.2}\right]}. \tag{9}$$

Fractional Efficiency Approach

Recent cyclone theories allow direct calculation of collection efficiency for particles of any size by cyclones of any design. The entire fractional efficiency curve can be determined without resorting to a generalized efficiency curve based on a critical diameter. Examples of this approach are the Leith–Licht (1972) theory and a newer theory by Dietz (1981).

Gas flow in industrial-sized cyclones is always turbulent. The Leith–Licht model accounts for turbulence by assuming that at any height in the cyclone, uncollected dust is completely and uniformly mixed. An average residence time in the cyclone is determined from cyclone dimensions and gas throughput. The resultant expression for collection efficiency is

$$\eta = 1 - \exp\left[-2(C\Psi)^{1/(2n+2)}\right]. \tag{10}$$

The influences of particle and gas properties are combined in Ψ, a modified inertia parameter:

$$\Psi = \frac{\rho_p d^2 v_i (n+1)}{18\mu D}. \tag{11}$$

The term C is a dimensionless geometry parameter that depends only on the eight cyclone dimension ratios. C is constant for any cyclone design, and each design has a unique value of C.

$$C = \frac{\pi D^2}{ab}\left[2\left\{1 - \left(\frac{D_e}{D}\right)^2\right\}\left(\frac{S}{D} - \frac{a}{2D}\right) + \frac{1}{3}\left(\frac{S+l-h}{D}\right)\left(1 + \frac{d_c}{D} + \frac{d_c^2}{D^2}\right) + \frac{h}{D} - \left(\frac{D_e}{D}\right)^2\frac{l}{D} - \frac{S}{D}\right]. \tag{12}$$

The natural length of the cyclone, l, was defined by Alexander (1949) as the farthest distance the spinning gas extends below the gas outlet duct.

$$l = 2.3 D_e \left(\frac{D^2}{ab} \right)^{1/3}. \quad (13)$$

The cone diameter at the natural length is

$$d_c = D - \frac{(D-B)(S+l-h)}{(H-h)}. \quad (14)$$

If the natural length exceeds $(H-S)$, l in Eqs. (12) and (14) is replaced by $(H-S)$.

The vortex exponent, n, describes the change in tangential gas velocity with radial position, r, in the cyclone: $v_t r^n = \text{constant}$. Experimental studies of cyclone flow patterns have measured n in the range of 0.5 to 0.9. Alexander (1949) presented an empirical expression to calculate n for any cyclone diameter and gas temperature.

$$n = 1 - \left[(1 - 0.67 D^{0.14})(T/283)^{0.3} \right]. \quad (15)$$

The Dietz (1981) model represents a refinement of the Leith–Licht method. The model divides the cyclone into three regions: the entrance region (the annular space around the outlet duct at the top of the cyclone); the downflow region (corresponding to the vortex below the level of the outlet duct); and the core region (formed by the extension of the outlet duct to the bottom of the cyclone). Turbulence is assumed to produce a uniform radial concentration profile for uncollected particles within each region. To approximate a distribution of particle residence times in the cyclone, the theory allows for the exchange of particles between the downflow and core regions. The Dietz model calculates cyclone collection efficiency as

$$\eta = 1 - \left[K_0 - \left(K_1^2 + K_2 \right)^{0.5} \right] \times \exp\left[\frac{-\pi (2S - a) \rho_p d^2 v_i}{18 \mu ab} \right]. \quad (16)$$

The subscripted K terms are functions of particle and gas properties as well as cyclone dimensions.

$$K_0 = \frac{1}{2}\left[1 + \left(\frac{D_e}{D} \right)^{2n} \left(1 + \frac{9\mu ab}{\pi \rho_p l d^2 v_i} \right) \right], \quad (17)$$

$$K_1 = \frac{1}{2}\left[1 - \left(\frac{D_e}{D} \right)^{2n} \left(1 + \frac{9\mu ab}{\pi \rho_p l d^2 v_i} \right) \right], \quad (18)$$

$$K_2 = \left(\frac{D_e}{D} \right)^{2n}. \quad (19)$$

As in the Leith–Licht theory, l should be replaced by $(H-S)$ if the natural length exceeds $(H-S)$; n can be calculated from Eq. (15).

EXPERIMENTS

All experiments were carried out on the test system shown in Figure 4. The cyclone was a Stairmand high-efficiency design with $D =$ 0.305 m. Room air was passed through an absolute filter that removed ambient particles. Gas flow was measured from the pressure drop across a calibrated Stairmand disc. Gas flowed past an upstream isokinetic sampling probe, through the cyclone, past a flow straightener and a downstream isokinetic sampling probe, and to the fan.

Accurate sampling of an aerosol directly downstream from the cyclone is difficult because the gas flowing from the cyclone is swirling. Techniques for sampling from swirling flow are available, but because of transient velocity patterns, these methods are difficult to use at best and unreliable at worst. To eliminate this problem, a flow straightener was installed in the cyclone outlet duct. The straightener was located three duct diameters downstream from the opening of the gas outlet duct, a distance sufficient to prevent any effect on flow patterns and collection efficiency within the cyclone (Shepherd and Lapple, 1939; Browne and Strauss, 1978).

The straightener was of the egg crate type with each cell $D/6$ in height, width, and depth, where D is the duct diameter. This straightener is reportedly very effective at

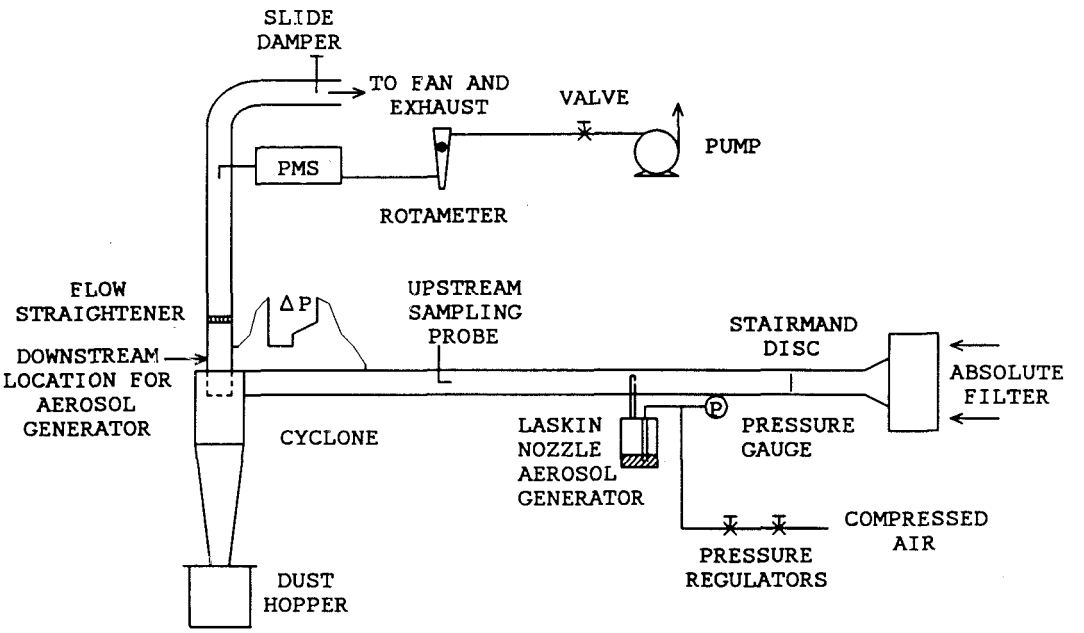


FIGURE 4. Schematic drawing of experimental cyclone system.

eliminating cyclonic flow (Ferguson et al., 1981). Our measurements confirmed that the gas velocity profile downstream of the straightener was flat and that the gas stream had negligible tangential velocity. The straightener also produced a uniform aerosol concentration profile in the downstream duct. Isokinetic samples taken at the duct centerline were found to be representative of the concentration and size distribution for the entire duct.

Because the flow straightener can collect particles that penetrate the cyclone, it is not possible to determine cyclone efficiency directly from a downstream aerosol sample. The combined efficiency of the cyclone and straightener can be measured by injecting particles into the duct upstream of the cyclone and sampling from the upstream and downstream probes in Figure 4.

$$\eta_{c+s} = 1 - \frac{N_{\text{up,down}}}{N_{\text{up,up}}}. \tag{20}$$

Here, N is the number of particles counted for any size, the first subscript is the location of the aerosol generator relative to the cyclone (up for upstream and down for downstream), and the second subscript refers to the sampling probe location.

The collection efficiency of the flow straightener can be measured directly by injecting aerosol downstream of the cyclone, but upstream of the straightener, at the location indicated in Figure 4. The concentration and size distribution of aerosol injected at this site are assumed identical to the concentration and size distribution of aerosol injected upstream of the cyclone as measured at the upstream sampling location. Because the operating parameters of the aerosol generator are not affected by its location, this is a reasonable assumption. The collection efficiency of the flow straightener is then

$$\eta_s = 1 - \frac{N_{\text{down,down}}}{N_{\text{up,up}}}. \tag{21}$$

The combined efficiency of the cyclone and flow straightener in series is related to the individual efficiency of each by

$$\eta_{c+s} = 1 - (1 - \eta_c)(1 - \eta_s). \quad (22)$$

By substituting Eqs. (20) and (21) into Eq. (22) and solving for η_c, cyclone efficiency can be expressed as

$$\eta_c = 1 - \frac{N_{\text{up,down}}}{N_{\text{down,down}}}. \quad (23)$$

Thus, cyclone efficiency can be measured by sampling the aerosol from a single location downstream of both cyclone and straightener while moving the aerosol generator between locations upstream and downstream of the cyclone, as indicated in Figure 4.

A *Laskin nozzle aerosol generator* (Laskin, 1948) was used to nebulize Arcoprime 200, a mineral oil with a density of 860 kg/m^3. The generator was operated at a compressed air pressure of 41.4 kPa (6.0 psig). This system was chosen because it produced spherical, liquid droplets that should not bounce or reentrain after striking the cyclone wall. Spherical particles and perfect collection are assumed by most efficiency theories. At both the upstream and downstream locations, aerosol was injected countercurrent to the air flow at the duct centerline via a cylindrical probe.

Isokinetic aerosol samples were taken through a 0.78-cm-diameter probe at the duct centerline downstream of the straightener. Particles were sized and counted with a Particle Measuring Systems (PMS, Inc., Boulder, CO 80301) aerosol scattering spectrometer. The maximum number concentration counted was 1.5×10^4/cm^3 without dilution, well below the concentration for which coincidence is significant for this single particle counter. The PMS was calibrated before the experiments with monodisperse latex spheres (Duke Scientific, Palo Alto, CA 94306) 2.02 and 4.1 μm in diameter. A second calibration after the tests showed no change in the response of the instrument.

The cyclone was tested at inlet velocities of 5, 10, 15, 20, and 25 m/s. The design inlet velocity for a Stairmand high-efficiency cyclone with $D = 0.305$ m is 15 m/s, based on an air flow of 0.139 m^3/s (300 cfm). Each inlet velocity was tested three times for a total of 15 experiments. For each test, ten samples were taken with the aerosol generator upstream of the cyclone (numerator in Eq. (23)) and ten samples were taken with the generator downstream (denominator in Eq. (23)). To minimize possible trends in aerosol generator output over time, the samples were taken in the following sequence: three upstream, five downstream, four upstream, five downstream, three upstream.

In each experiment, all particles ≥ 1 μm in diameter were counted and sized by the PMS into intervals of width 0.75 μm. Cyclone efficiency for the midpoint of each size interval was calculated from Eq. (23), where $N_{\text{up,down}}$ and $N_{\text{down,down}}$ were the average number of counts for the ten replicate samples.

Cyclone pressure drop was measured at each inlet velocity. The downstream pressure taps were located between the cyclone and the flow straightener so that only losses due to the cyclone were included. Two taps, 90 degrees apart, were sufficient to give an accurate static pressure measurement in the swirling gas flow. The upstream pressure tap was in the 0.15 m (6-inch) diameter duct, ahead of the round-to-rectangular transition to the cyclone inlet. Transition losses calculated by standard methods (ACGIH, 1980) were minimal. Since the duct areas were the same at both taps, there were no velocity pressure differences between inlet and outlet and the measured cyclone pressure differential reflected static losses only.

RESULTS AND DISCUSSION

Cyclone pressure drop values for each of the five air flows tested are presented in Table 2. Energy loss in cyclones is commonly expressed as a number of gas inlet velocity heads, ΔH. For any cyclone design, ΔH should be constant for all inlet velocities.

TABLE 2. Experimental Cyclone Pressure Drop

Inlet velocity (m/s)	Pressure drop (Pa)
5.1	87
10.0	336
15.0	785
20.0	1407
25.0	2205

Division of the pressure drop values in Table 2 by $(\rho_g v_i^2)/2$ gives an average ΔH of 5.7 for the Stairmand high-efficiency cyclone. This is slightly higher than the value of 5.3 that we calculated from the data that Stairmand (1951) reported for this design.

Figure 5 shows the experimental fractional efficiency curves for all cyclone inlet velocities. Each point represents the mean cyclone efficiency for three tests. The effects of particle diameter and cyclone inlet velocity on efficiency are in general agreement with theoretical predictions. For any diameter, Figure 5 shows that efficiency increases with inlet velocity. For any inlet velocity, efficiency increases with particle diameter.

Stairmand's (1951) fractional efficiency curve for this design was determined under experimental conditions different from ours: $D = 0.203$ m; $\rho_p = 2000$ kg/m^3; $v_i = 15.2$ m/s. To compare his data with our curve for $v_i = 15$ m/s, it is necessary to make the following transformation (Stairmand, 1951):

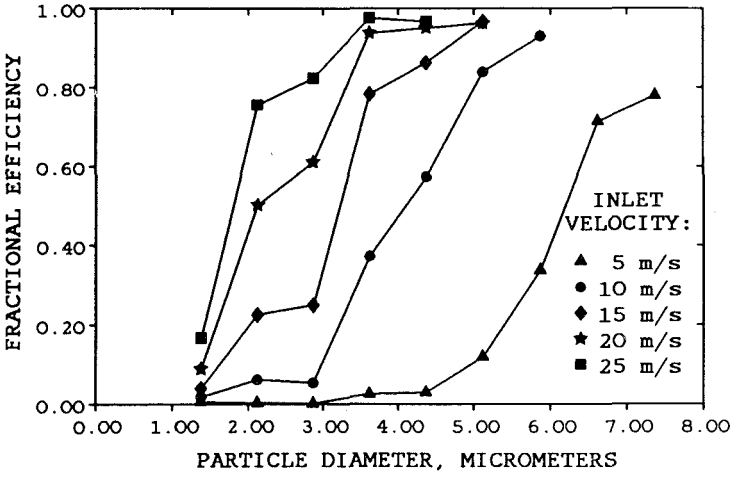
$$d_2 = d_1 \sqrt{\frac{\rho_{p1} v_{i1} D_2}{\rho_{p2} v_{i2} D_1}} . \tag{24}$$

Here d_1 is the particle diameter collected at a given efficiency under Stairmand's operating conditions (subscript = 1); d_2 is the particle diameter that will be collected with the same efficiency when Stairmand's results are converted to our experimental conditions (subscript = 2).

Figure 6 shows the results of this transformation. In our experiments, collection efficiency was higher for particle diameters larger than ≈ 3.5 μm. This discrepancy may be partly explained by differences in aerosols. The liquid droplets used here should be collected upon hitting the cyclone wall. In contrast, the solid particles used in Stairmand's tests might bounce or reentrain after striking the wall and pass through the cyclone, lowering efficiency. This effect is more likely to occur for large particles.

For smaller particles, Stairmand's results show a higher efficiency than we obtained. It is well known that high inlet dust concentrations can result in increased cyclone efficiency

FIGURE 5. Experimental fractional efficiency curves for Stairmand high-efficiency cyclone at inlet velocities from 5 m/s to 25 m/s.



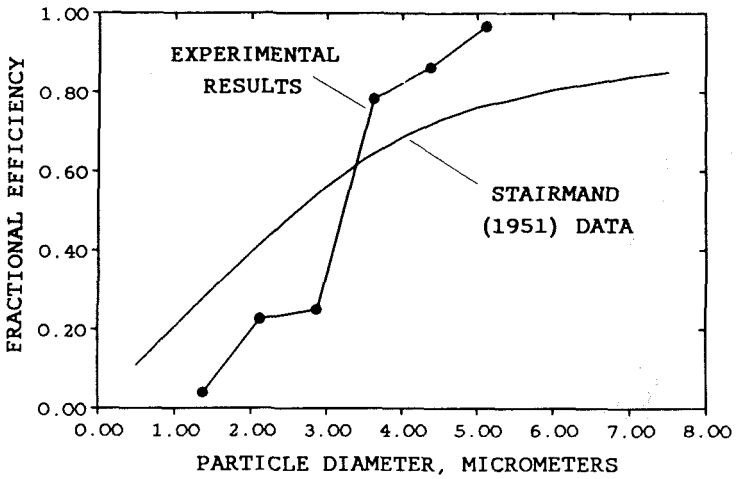


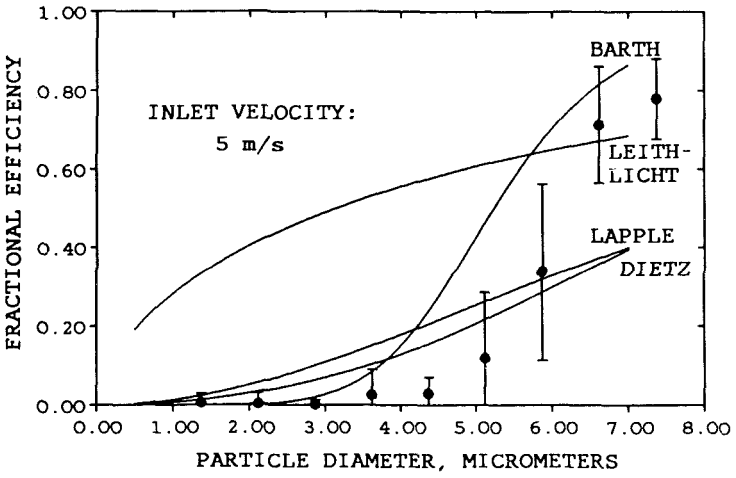
FIGURE 6. Comparison of experimental fractional efficiency for Stairmand high-efficiency cyclone at inlet velocity = 15 m/s with Stairmand's (1951) curve; Stairmand's data have been transformed to our experimental conditions by Eq. 24.

FIGURE 7. Experimental and theoretical efficiency for Stairmand high-efficiency cyclone at inlet velocity = 5 m/s; for Figures 7–11, solid lines indicate theoretical predictions, data points are mean results for three experiments, and error bars represent 95% confidence intervals.

due to particle agglomeration and to large particles sweeping smaller ones out of the gas stream. Based on an extensive review of experimental data, Stern et al. (1955) presented the following relationship between dust concentration and collection efficiency:

$$\frac{1-\eta_1}{1-\eta_2} = \left[\frac{c_{i2}}{c_{i1}}\right]^2. \tag{25}$$

This equation predicts a decrease in cyclone penetration of approximately 35% for a tenfold increase in dust concentration; for a 100-fold increase in concentration, a 60% decrease in penetration is predicted. There



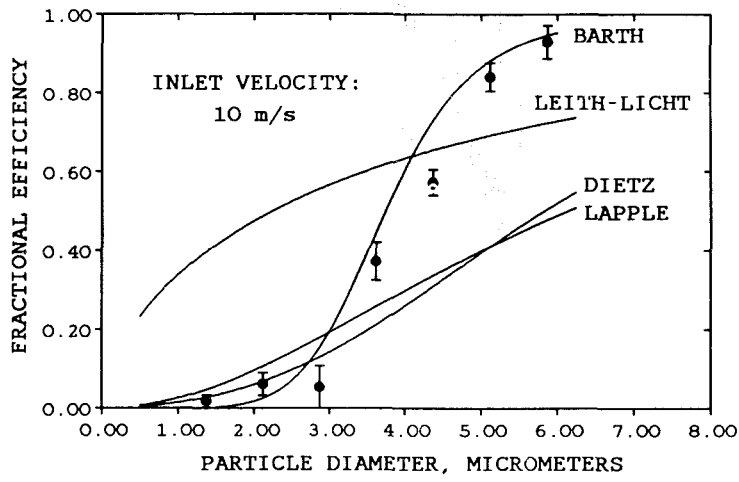
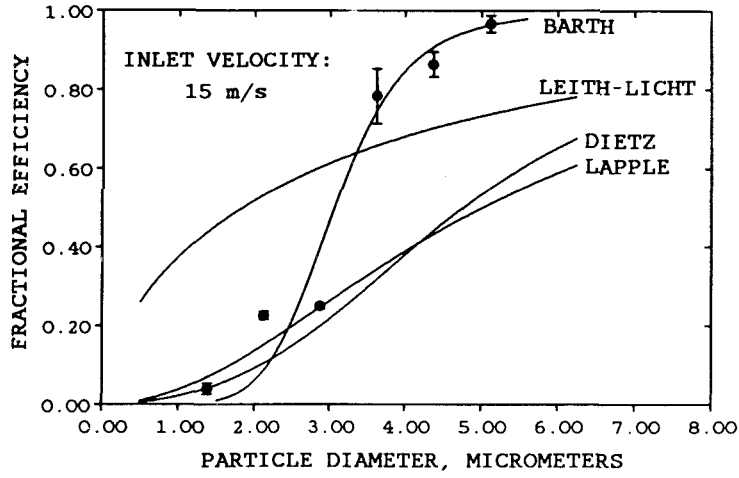


FIGURE 8. Experimental and theoretical efficiency for Stairmand high-efficiency cyclone at inlet velocity = 10 m/s.

was considerable variability in the data that Stern et al. (1955) reviewed, and the exponent for (c_{i2}/c_{i1}) ranged from 0.05 to 0.5. Our highest mass inlet concentrations were in the range of 50 mg/m^3 where interactions between particles are unlikely. The concentrations in Stairmand's experiments were not explicitly stated; however, Appendix II to Stairmand (1951), which describes standard cyclone testing procedures, indicates that inlet concentrations of 5 to 10 g/m^3 were normally used. A difference in inlet concentrations of this magnitude could explain the higher collection efficiency that Stairmand observed for small particles.

Figures 7 through 11 compare experimental results with the predictions of cyclone efficiency theories. Each plot shows test results for a single inlet velocity. The theoretical predictions are represented by smooth curves. (Note that the curves based on Barth's

FIGURE 9. Experimental and theoretical efficiency for Stairmand high-efficiency cyclone at inlet velocity = 15 m/s.



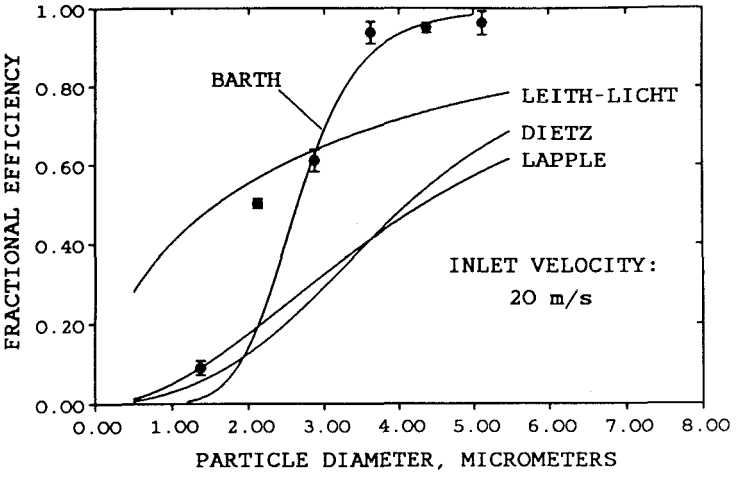


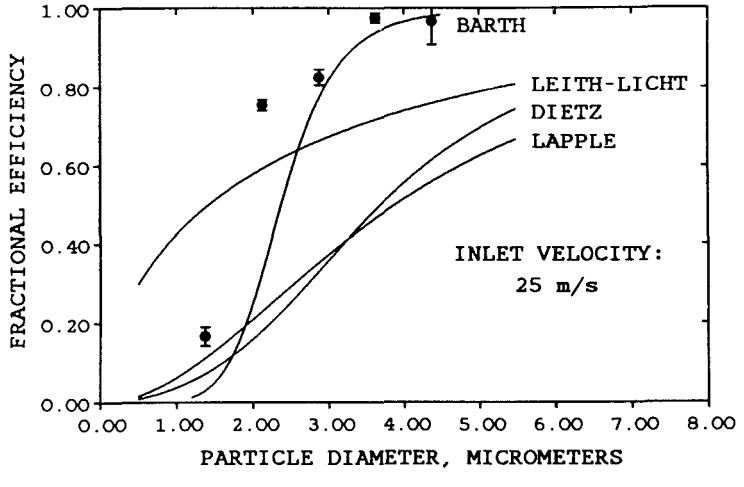
FIGURE 10. Experimental and theoretical efficiency for Stairmand high-efficiency cyclone at inlet velocity = 20 m/s.

theory have been modified as described below.) Results are plotted as the mean efficiency for the three tests with 95% confidence intervals around the mean.

It is apparent from Figures 7 through 11 that with the exception of the modified Barth theory, none of the theoretical efficiency curves fits the data well. The Lapple theory, except for small particle diameters and low inlet velocities, considerably underestimates efficiency. This lack of agreement is not surprising since Lapple's value of $N = 5$ was used for the number of gas stream revolutions in the cyclone.

Lapple intended for N to be an adjustable parameter that could be used to "calibrate" theoretical predictions, based on experimental results. We can do this by determining d_{50} from the experimental fractional efficiency curves and then solving Eq. (1) for N, but there are two problems with this

FIGURE 11. Experimental and theoretical efficiency for Stairmand high-efficiency cyclone at inlet velocity = 25 m/s.



approach. First, N does not appear to be a uniform function of cyclone design, but instead increases with inlet velocity. For our data, N is ≈ 10 to 12 for inlet velocities up to 15 m/s. Cut diameters at the two highest inlet velocities are consistent with $N \approx 20$ to 25. Since the choice of N is unclear even after calibration, the predictive value of the Lapple method is limited.

If N is determined by this calibration procedure, the theoretical Lapple curves in Figures 7 through 11 will be shifted upward. The fit to the data is improved, but still not ideal, since the shape of the theoretical curves is determined by Lapple's relationship of efficiency versus d/d_{50} (Figure 2, Eq. (2)). The Lapple curves are flatter than the data; matching efficiency at the cut diameter results in overestimation of efficiency for small sizes and underestimation for particles larger than d_{50}.

The predictions of the Dietz theory fall in the same range as the Lapple curves in Figures 7 through 11. Experimental cyclone efficiency is much higher than predicted by the Dietz theory, except for small particle diameters at inlet velocities of 5 and 10 m/s. The only adjustable parameter within the Dietz theory is the vortex exponent, n. Theoretical curves were calculated using $n = 0.56$, obtained from Eq. (15), although Dietz (1981) uses $n = 0.7$. Higher values of n indicate higher tangential velocity in the vortex and greater centrifugal force acting on particles in the gas stream, so increasing n to 0.7 would increase predicted efficiencies. However, for the Stairmand high-efficiency-cyclone, the predictions of the Dietz theory are not very sensitive to changes in n and the upward shift in the efficiency curves would be slight.

The theoretical curves based on the Leith–Licht cyclone model predict higher collection efficiency than either the Lapple or Dietz models. For all inlet velocities, the Leith–Licht curves intersect the experimental data at fractional efficiencies slightly higher than 0.5. Since the Leith–Licht curves are flatter, this model underestimates efficiency for most particle diameters larger than d_{50}. For smaller particles, the model greatly overestimates cyclone efficiency. Like the Dietz theory, the Leith–Licht theory has no easily adjustable parameters other than n; changes in n over the normal range of this parameter have only a small effect on predicted efficiency.

The Leith–Licht theory assumes that turbulence in the cyclone is sufficient to cause complete radial back-mixing of uncollected particles in any plane perpendicular to the cyclone axis. The Dietz theory assumes uniform radial concentration profiles in each of the three cyclone regions that it defines. This, in part, accounts for the relatively flat theoretical efficiency curves calculated by the two models. The steeper slopes of the experimental curves suggest that the effects of turbulence are less than predicted. Measurements have shown that there is a concentration gradient for particles in the vortex of a cyclone. Mothes and Loffler (1982) found that larger-particle (≈ 3.5 μm) concentrations were much higher near the cyclone wall and decreased by nearly two orders of magnitude from the wall to the cyclone core. Smaller-particle (≈ 0.5 μm) concentrations were much more uniform as radial position changed. Hejma (1971) found similar results for large particles throughout the cyclone. Small (1–2 μm) particles had lesser concentration gradients in the cone, and in the cylinder, concentration was almost independent of radial position. These studies indicate that the assumptions of complete radial back-mixing made by the Leith–Licht and Dietz theories are not justified, at least for larger particles. Smaller particles, with less centrifugal force, might be more strongly influenced by turbulence.

Of the four cyclone theories, only the fractional efficiency curves calculated by the Barth theory matched the steep slope of the experimental data. However, these curves were positioned far to the right of the experimental curves. We found that using the

terminal settling velocity ratio calculated by Eq. (4) as an adjustable parameter produced better results. For any particle diameter, v_{ts}/v_{ts}^* calculated from Eq. (4) was quadrupled. This higher value was then used with Figure 3 or Eq. (9) to determine the efficiency for that particle size. The Barth curves in Figures 7 through 11 are based on this modification and agree reasonably well with experimental fractional efficiency data for most inlet velocities. The modified Barth theory underpredicted efficiency at 25 m/s and overpredicted at 5 m/s. Overall, the modified Barth theory provides a better fit to the data than the methods of Leith–Licht, Dietz, or Lapple.

The success of this adjustment indicates that although the value of v_{ts}^* calculated by the Barth theory is incorrect, the shape of Barth's curve of efficiency versus v_{ts}/v_{ts}^* is adequate for the Stairmand high-efficiency cyclone. Barth's generalized efficiency curve was developed from experiments with several cyclone designs and probably represents the average performance of all of these designs. Others (Petroll et al., 1967; Loffler, 1970) have found that the shape of such a curve depends on cyclone configuration and that no single curve should be considered valid for all designs. Thus, the applicability of Barth's theory (as modified here) to other designs is uncertain.

SUMMARY AND CONCLUSIONS

Collection efficiency for a Stairmand high-efficiency cyclone was measured under carefully controlled experimental conditions. An aerosol of liquid droplets was used to minimize the possibility of particle reentrainment after collection in the cyclone and to provide the spherical particles assumed by cyclone efficiency theories. Predictions of four theories, representing three different approaches for calculating collection by a cyclone, were compared with the data.

As presented in the literature, none of the theories predicted experimental cyclone efficiency accurately. Although the Lapple theory underestimated efficiency, this theory contains a parameter that can be adjusted to produce better agreement between theoretical predictions and results. Since the results must be known before the adjustment can be made, and since the adjustment appears to depend on cyclone inlet velocity, the predictive value of the theory is limited. The Dietz theory consistently underpredicted efficiency and contains no easily adjusted parameters.

The predictions of the Leith–Licht theory were closer to experimental results than those of the Lapple or Dietz methods, although the shape of the theoretical fractional efficiency curves did not match the data. Theoretical curves were flatter, crossing the experimental curves at a particle size slightly larger than the cut diameter. Only the curves predicted by the Barth theory were as steep as the experimental curves. An empirical adjustment to the terminal settling velocity ratio was required to shift the theoretical curves into proper position, since the unmodified theory predicted cut diameters roughly twice as large as measured values. After this adjustment, the Barth theory provided the best fit to the experimental data.

Although the modified Barth and Leith–Licht theories worked best for the Stairmand high-efficiency cyclone, this conclusion may not apply to other cyclone designs. Design changes alter gas flow patterns in the cyclone, and theoretical assumptions and simplifications that work well for one design may not be valid for another. The theories need to be evaluated over a range of cyclone designs and operating conditions.

In spite of these problems, efficiency theories may be adequate for many practical applications. Our experiments looked at fractional efficiency for particles smaller than 10 μm. In this size range, discrepancies among theories and differences between results and predictions are greatest. Often, one is more interested in the overall, or integrated, mass efficiency of a cyclone on dusts that are composed mainly of particles larger than

10 μm in diameter. Theoretical predictions are likely to be closer to results in these situations.

This work was supported by grant CPE-8012968 from the National Science Foundation. We are grateful for the valuable comments and suggestions of our colleagues, Drs. Douglas Cooper, Michael Ellenbecker, and Henry Feldman.

REFERENCES

Alexander, R. McK. (1949). *Proc. Australas. Inst. Min. Metall. (New Series)* 152–153:203.

American Conference of Governmental Industrial Hygienists. (1980). *Industrial Ventilation: A Manual of Recommended Practice* (16th ed.). ACGIH Committee on Industrial Ventilation, Lansing, Mich.

Barth, W. (1956). *Brennst. Waerme Kraft* 8:1.

Browne, J. M., and Strauss, W. (1978). *Atmos. Environ.* 12:1213.

Dietz, P. W. (1981). *A.I.Ch.E.J.* 27:888.

Ferguson, B. B., Mitchell, W. J., Reece, J. W., and Sterret, J. D. (1981). Paper no. 81-7.6 in *74th Air Pollution Control Association Annual Meeting.*

Hejma, J. (1971). *Staub-Reinhalt. Luft* 31, 7:22.

Jackson, R. (1963). *Mechanical Equipment for Removing Grit and Dust from Gases.* Cheney and Sons, Banbury, England.

Lapple, C. E. (1950). *Ind. Hyg. Q.* 11:40.

Laskin, S. (1948). *Submerged Aerosol Unit: AEC Project Quarterly Report UR-38.* University of Rochester, Rochester, N.Y.

Leith, D., and Licht, W. (1972). *A.I.Ch.E. Symp. Ser.* 68:196.

Leith, D. (1979). In *Handbook of Environmental Engineering* (N. C. Pereira and L. K. Wang, eds.). Humana Press, Clifton, N.J., Vol. I, p. 61.

Loffler, F. (1970). *Staub-Reinhalt. Luft* 30, 12:1.

Mothes, H., and Loffler, F. (1982). *J. Aerosol Sci.* 13:184.

Petroll, J., Quitter, V., Schade, G., and Zimmermann, L. (1967). *Staub-Reinhalt. Luft* 27, 3:1.

Shepherd, C. B., and Lapple, C. E. (1939), *Ind. Eng. Chem.* 31:972.

Stern, A. C., Caplan, K. J., and Bush, P. D. (1955). *Cyclone Dust Collectors.* American Petroleum Institute, New York.

Stairmand, C. J. (1951). *Trans. Inst. Chem. Eng.* 29:356.

Swift, P. (1969). *Steam Heat. Eng.* 38:453.

Theodore, L., and DePaola, V. (1980). *J. Air Pollut. Control Assoc.* 30:1132.

Received 5 October 1984; accepted 6 March 1985